Journal of Materials Chemistry A

COMMUNICATION

View Article Online
View Journal

Cite this: DOI: 10.1039/c5ta10316a

Fluidized bed electrodes with high carbon loading for water desalination by capacitive deionization†

G. J. Doornbusch,[ab] J. E. Dykstra,[bc] P. M. Biesheuvel[bd] and M. E. Suss*[a]

Received 16th December 2015
Accepted 19th January 2016

DOI: 10.1039/c5ta10316a

www.rsc.org/MaterialsA

The use of carbon flow electrodes has significantly impacted electrochemical energy storage and capacitive deionization (CDI), but device performance is limited as these electrodes cannot surpass ~20 wt% carbon while maintaining flowability. We here introduce flowable fluidized bed electrodes which achieve up to 35 wt%, and apply these to water desalination by CDI.

Introduction

Water desalination by capacitive deionization (CDI) is a fast emerging technology, with tremendous advances over the past half-decade.[1] The basic phenomena underpinning CDI technology is ion electrosorption into micropores, whereby salt ions are stored electrostatically in electric double layers (EDLs) formed within micropores of charging porous carbon electrodes. The traditional CDI cell consists of two static porous carbon electrodes sandwiching the feed flow channel. Transferring electrons between the two electrodes via an external power supply allows for desalting the flowing feedwater. Once the cell is fully charged, the electrodes must be regenerated, which is often accomplished by shorting the two electrodes, resulting in a brine cell effluent.

One of the most promising recent advances in CDI is the advent of flow electrode capacitive deionization (FCDI). In FCDI, traditional static (or film) electrodes were replaced by flow electrodes consisting of suspensions of micron-scale carbon particles in an electrolyte.[2] The latter advance was preceded by the use of flow (or slurry) electrodes in electrochemical energy storage systems such as flow batteries[3] and supercapacitors,[4] and the decades-old investigations of such flow electrodes.[5] The two main advantages of FCDI compared to CDI are that FCDI enables continuous desalination with a single cell, as electrode regeneration can occur downstream of the cell, and FCDI can also desalinate significantly higher salinity feeds than CDI.[2]

One major limitation of FCDI is the poor electronic conductivity of the flow electrodes, reported to be of order 0.1–1 mS cm^{-1},[6] which is the result of transporting electric charge through a discontinuous network of carbon particles. This conductivity is many orders of magnitude lower than that achieved by static electrodes,[7,8] and on the order or lower than the ionic conductivity of typical feedwaters. Thus, transporting electronic charge through the electrode is a major bottleneck for FCDI technology, limiting the achievable salt removal rate and cell energy efficiency.[6] Similarly, low electronic conductivity has been reported for the carbon flow electrodes of flow batteries,[9] flow supercapacitors,[10] and flow electrode Capmix systems.[6]

It has been demonstrated previously that flow electrode electronic conductivity is a strong function of the electrode's carbon weight percentage (CWP, expressed in wt%), as increasing this percentage enables more effective electronic charge percolation.[6,9] Thus, one clear pathway to achieve the needed breakthrough in flow electrode performance is to increase the CWP. However, until now, the practical CWP of flow electrodes has been limited to about 20 wt% as more concentrated electrodes are no longer flowable.[6,11] Another challenge for FCDI is operating the cell continuously while regenerating and re-using the electrodes in a closed-loop manner. Current strategies involve adding system components, such as two FCDI cells in series (one for charging the carbon particles, another for discharging the particles),[12] or an extra (a third) ion exchange membrane to separate the desalted and brine streams.[13]

In this work, we demonstrate a breakthrough in suspension electrodes, achieving a flowable electrode with up to 35 wt% by leveraging upflow fluidized bed electrodes. The unique properties of fluidized beds allow us to overcome the limitations of previously used flow electrodes. Crucially, we show flowable,

[a]Faculty of Mechanical Engineering, Technion – Israel Institute of Technology, Haifa, 32000, Israel. E-mail: mesuss@technion.ac.il

[b]Wetsus, European Centre of Excellence for Sustainable Water Technology, Oostergoweg 9, 8911 MA Leeuwarden, The Netherlands

[c]Department of Environmental Technology, Wageningen University, Bornse Weilanden 9, 6708 WG Wageningen, The Netherlands

[d]Laboratory of Physical Chemistry and Soft Matter, Wageningen University, Dreijenplein 6, 6703 HB Wageningen, The Netherlands

† Electronic supplementary information (ESI) available. See DOI: 10.1039/c5ta10316a

exceptionally high CWP beds in our electrode compartment while simultaneously the CWP in the surrounding flow system remains very low (here ~2.5 wt%), thus preventing clogging of the flow system and minimizing pumping requirements. We further demonstrate the first use of fluidized bed electrodes for water desalination by CDI, and termed this novel technology "fluidized bed capacitive deionization" (Fbed CDI). We show that our Fbed CDI cell can continuously desalinate feedwater for several days while using a novel, low infrastructure, and robust closed-loop system to regenerate and re-use the electrodes.

Fig. 1 is a schematic depiction of our Fbed CDI cell in comparison to typical FCDI cells. Flow electrodes typically employ smaller, order 10 μm sized carbon particles,[2,14,15] and the particles are entrained by the electrolyte and travel at the electrolyte's velocity.[10] By contrast, the fluidized bed electrode contains larger (>100 μm diameter), spherical carbon beads and flow is against the direction of gravity. As a result of the relatively large bead size, gravitational forces acting on the beads can significantly retard the particle relative to the flowing electrolyte, leading to densely packed flowing suspensions in the electrode compartments.[16] The influence of particle size can be quantitatively captured by the non-dimensional Archimedes number, which is the ratio of gravitational to viscous forces acting on a carbon particle,

$$\mathrm{Ar} = d_\mathrm{p}^{\,3}\rho(\rho_\mathrm{p} - \rho)g/\mu^2 \quad (1)$$

where d_p is the carbon particle diameter, ρ is the electrolyte density (approximately that of water), ρ_p is the density of the porous particle when filled with the electrolyte, g is the gravitational acceleration, and μ is the electrolyte viscosity. For standard flow electrodes, where the typical carbon particle size is of order 10 μm, the Archimedes number is either zero (for horizontal flow) or order 0.001 (for vertical flow). In comparison, Fbed CDI systems are designed for Archimedes numbers of order unity and above, by ensuring that flow is against gravity and using large enough beads, here order 100 μm diameter. Another unique feature of fluidized beds is that the carbon bead volume fraction (and also CWP) is not a static value as in flow electrodes, but a function of the relative velocity between the particle and liquid. For sedimentation, this relationship is often described by the empirical Richardson–Zaki relation,[16]

$$U_\mathrm{p} - U_\mathrm{w} = U_\mathrm{T}(1 - \phi)^{n-1} \quad (2)$$

where U_p is the local particle velocity, U_w is the local electrolyte velocity, U_T is the terminal velocity of a single sedimenting particle, ϕ is the particle volume fraction in the bed, and n is an empirically determined parameter ($n \sim 4.65$ for sedimentation in the creeping flow regime with smooth spherical particles).[16]

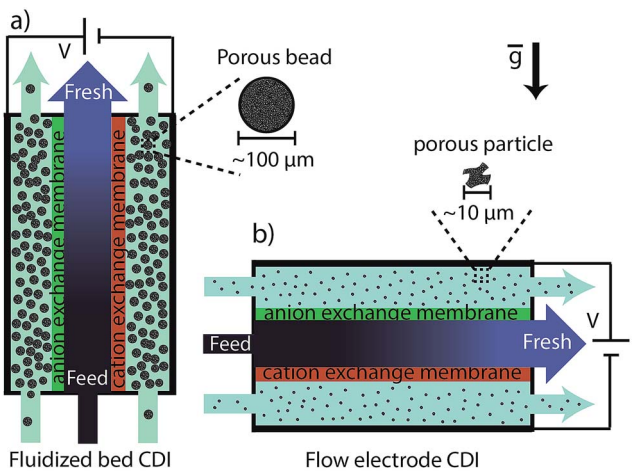

Fig. 1 Schematics of (a) the fluidized bed CDI (Fbed CDI) cell, compared to (b) a flow electrode CDI (FCDI) cell. While both technologies utilize flowing carbon suspensions as electrodes, FCDI is characterized by a negligible effect of gravity on the small carbon particles in the cell, and a maximum electrode carbon wt% (CWP) of ~20%. Fbed CDI is characterized by a significant gravitational effect on the large carbon beads, enabling a densely packed fluidized bed electrode with CWP up to 35 wt%, and simultaneously low CWP (~2.5 wt%) in the surrounding flow system.

Experimental methods

The Fbed CDI cell consisted of graphite current collectors, acrylic endplates, and ion exchange membranes (Neosepta IEM and CMX, Tokuyama, Japan). Recesses of 20 by 112 mm were milled into the acrylic endplates and the graphite current collector was press fit into the recesses, leaving a gap of 1 mm in the acrylic above the current collector. 1.5 mm thick silicon gaskets were placed on the top of the acrylic layers with a hole cut into them of 20 by 112 mm. The latter assembly formed the electrode compartment, and each electrode compartment, after cell compression for sealing, was ~2.4 mm thick. Ion exchange membranes served as the inner wall of the electrode compartments and the outer wall of the feed channel. The feed flow compartment had the same area as the electrode compartments, and was cut into a 0.22 mm thick silicon gasket. The cell was sealed with ten M6, 50 mm long stainless steel bolts, and connection to an external power supply was made with titanium M6, 40 mm long bolt threaded into the outside surface of the acrylic endplates to contact the outside of the current collector.

A separate setup, which we termed the "optically accessible compartment", was constructed to measure the CWP in the fluidized bed electrode. This setup consisted simply of a single acrylic endplate with a milled channel for the electrode, at least one silicon gasket with a cut hole forming part of the electrode compartment (or an o-ring serving the same purpose), and a second acrylic endplate to seal the electrode compartment and allow for optical access into the cell. The electrode compartment area was the same as that used in the Fbed CDI cell, and its thickness was varied between 1.2 and 6.4 mm in order to test the effect of compartment thickness on the fluidized bed electrode composition.

The fluidized bed electrode utilized activated carbon beads (TE-3 activated carbon beads, Mast Carbon International Ltd., United Kingdom), where the bead size ranged between 125 and 250 μm in diameter. The beads have significant microporosity,[17] and so are appropriate as high performance CDI electrodes.

Before use, the beads were wetted and placed on a 75 μm sieve (Cole Parmer, USA) to filter out any small carbon particles. Then, water was poured onto the sieve, filling the sieve and catch pan, causing most beads to sink to the sieve surface. Other beads did not sink, remaining instead above the sieve surface as their pore structure remained filled with air. This process was repeated two more times, and after the third time, any remaining beads which did not sink were skimmed off the top and discarded. The remaining beads were then dried for 24 h at 105 °C before use.

The full system used in desalination experiments is shown in Fig. 2. A feed solution of 20 mM NaCl was pumped through the cell's feed channel by using a peristaltic pump (Cole Parmer, USA) at either 0.5 or 1.5 mL min^{-1} flow rate. Desalted water emerged from the cell, and a conductivity sensor (Metrohm 856, $K = 0.7$ cm^{-1}) was placed at the exit to measure the desalted water conductivity. The two current collectors were connected via a Keithley 2400 power supply (Keithley Instruments Inc., USA) which set a constant voltage difference between them. The voltage used varied from 1.0 to 1.9 V, and the resulting current was between ~3 A m^{-2} and 8 A m^{-2} (area used is that of a single electrode compartment in the cell). A mixing vessel was made from a 57 mm inner diameter PVC pipe, and this held the carbon suspension. The initial suspension (before operation of the cell) consisted of 200 mL of 20 mM NaCl and 18.2 g carbon (8.3 wt%). The contents of the mixing vessel were continuously stirred using a mixer at 300 rpm (Eurostar 60 Digital, IKA, USA) in order to prevent bead sedimentation and ensure a fairly uniform bead concentration in the tank. A peristaltic pump was used to pump the electrodes from the mixing vessel into the two electrode compartments with a flow rate for each electrode of 2.5 mL min^{-1}, using 1.6 mm inner diameter norprene tubing (Saint Gobain, France).

After passing through the charging cell, the suspensions consisted of charged beads with electrosorbed salt ions, and the beads needed to be discharged before re-use. The charged suspension was returned to the mixing vessel, where the beads spontaneously discharged and released salts via mutual collisions in the stirred tank. The latter resulted in an increase of the conductivity of the tank electrolyte, which was intermittently measured by a second conductivity sensor placed in the tank (Metrohm 856, Switzerland, $K = 0.7$ cm^{-1}), see Fig. 5, red triangles. To take these conductivity measurements, the mixer would be stopped for 60 s to allow the beads to temporarily sediment away from the conductivity sensor in the mixing vessel. Thus, the mixing vessel served several purposes, including housing the uncharged carbon beads, regenerating used electrode beads, and holding the brine. In order to prevent the unchecked increase of the brine salt concentration (and hence the concentration of the electrolyte in the fluidized bed electrode), a small part of the feedwater stream was continuously pumped into the mixing vessel at 0.15 mL min^{-1}. To remove brine from the tank for discard, an overflow section was created in the mixing vessel. The overflow section was fed by a thin 8 mm inner diameter and 155 mm length vertical tube, which allowed for the separation of brine from beads due to the stagnant (unstirred) condition in the vertical tube. As feedwater was pumped into the mixing vessel, brine was forced up the vertical tube and into the overflow compartment, while beads remained in the mixing vessel.

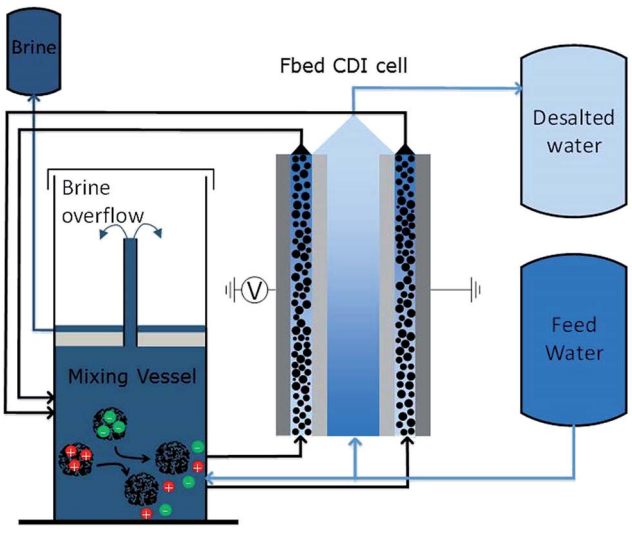

Fig. 2 Schematic of the Fbed CDI system for continuous desalination and closed-loop electrode regeneration and re-use. The suspension is pumped from the mixing vessel into the electrode compartments, forming fluidized bed electrodes. In the cell, the carbon beads are charged and electrosorb salt ions. The charged beads are then returned to the mixing vessel where they spontaneously release salts via discharging collisions. A small flow of feed water into the mixing vessel pushes brine into the brine overflow compartment, while the beads remain in the mixing vessel.

Results and discussion

In Fig. 3, we show the rise of the fluidized bed as it initially enters the optically accessible compartment. The pictures are sequential in time, with (a) showing the initial entrance of beads from the bottom of the compartment, (b) showing the rise of the dense fluidized bed characterized by a clearly observable bed rise height, and (c) showing the completed upflow fluidized bed, with beads leaving from the compartment

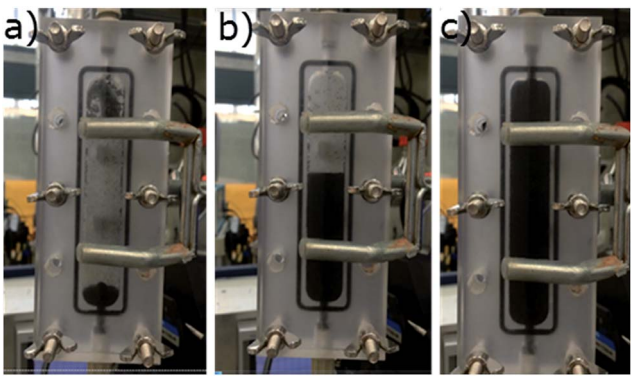

Fig. 3 (a–c) are pictures of the rise of the fluidized bed in the optically accessible compartment, and are sequential in time, with (a) occurring earliest followed by (b) and then (c).

through the top of the compartment. Once the bed fills the compartment, as in (c), it will remain formed as long as the suspension is pumped into the compartment, and in this state can be used for water desalination by Fbed CDI. As can be seen from Fig. 3b, the growth of the fluidized bed is characterized by a kinematic shock (a sharp discontinuity in bead density) where above the shock there is a complete absence of beads. For such a shock, the upward velocity of the shock is equal to the local velocity of the beads,[18] and thus the observed bed rise (shock) velocity can be used to calculate the bead volume fraction in the fluidized bed, ϕ_{bed}. This is accomplished by a conservation of the bead volumetric flux between the cell and upstream tubing,

$$\phi_{bed} = \phi_{in} Q / U_p A \quad (3)$$

where Q is the total suspension flow rate set by the pump, A is the electrode flow cross-sectional area, and U_p is the measured bed rise velocity (the local carbon particle velocity, see ESI† for more details on U_p measurements). Also, ϕ_{in} is the measured volume fraction of beads in the inflow tubing. In each case, ϕ_{in} was ~5 vol%, translating to a CWP of about 2.5 wt%, see ESI† for more details on these measurements. Subsequently, ϕ_{bed} was converted to CWP using

$$\mathrm{CWP} = \frac{\phi_{bed}(1-p)\rho_c}{\phi_{bed}\rho_p + (1-\phi_{bed})\rho} \quad (4)$$

where ρ_c is the mass density of the carbon phase ("skeleton density", $\rho_c = 1.7$ g mL^{-1}), ρ_p is the density of the electrolyte filled carbon particle ($\rho_p = 1.23$ g mL^{-1}), ρ is the density of water ($\rho = 1$ g mL^{-1}), and p is the bead porosity ($p = 0.67$, see ESI† for details).

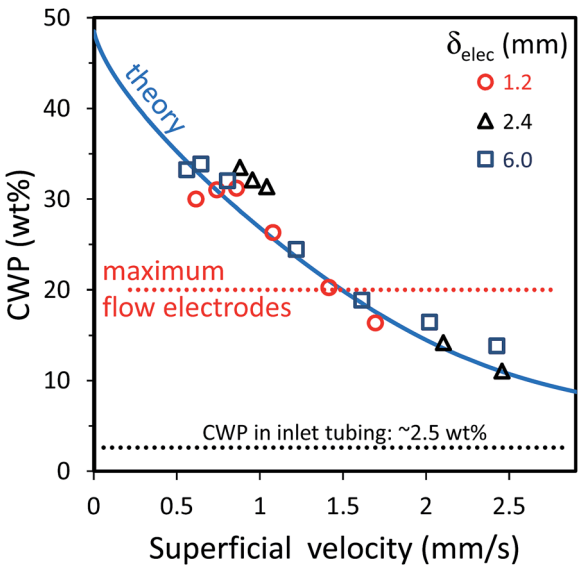

Fig. 4 Plot of the measured carbon weight percentage (CWP) of the fluidized bed versus bed superficial velocity, U_{sup} for various compartment thicknesses, δ_{elec}. The experimental data were fitted to the Richardson–Zaki equation (blue curve). Results demonstrate that fluidized bed electrodes can reach up to 35 wt% while maintaining electrode flowability. Simultaneously, the CWP of the flow entering the compartment remains low (~2.5 wt%).

In Fig. 4, we plot the experimentally measured electrode CWP (eqn (4)) versus the electrode superficial velocity, U_{sup} ($U_{sup} = Q/A$), for varying electrode compartment thicknesses, δ_{elec}, including 1.2, 2.4 and 6.0 mm. We fit the data in Fig. 4 to the Richardson–Zaki equation (eqn (2)), and find that the data are largely consistent with this equation for a best-fit exponent $n \sim 1.1$, and coefficient $U_T \sim 2.5$ mm s^{-1} (blue curve in Fig. 4, see ESI† for a discussion on this fitting). From Fig. 4, we observe that the fluidized bed exhibits a higher CWP at lower U_{sup}, while the CWP does not vary significantly with δ_{elec}. The maximum CWP obtained is about 35 wt% at the lowest flow rates tested, indicating that fluidized bed electrodes can attain CWPs of nearly twice the limit of FCDI flow electrodes while remaining flowable.

In Fig. 5, we show a representative result for the desalination performance of our Fbed CDI system, in the form of NaCl concentration versus time. Here we used the system shown in Fig. 2, and apply a voltage of 1.6 V between the two electrodes from $t = 0$ onward (resulting cell current is shown in Fig. S1†). The electrode flow rate was $Q = 2.5$ mL min^{-1} (so 5 mL min^{-1} for both electrodes), and the feed flow rate was 0.5 mL min^{-1}. The dotted line represents a constant feed concentration of 20 mM which flows into the cell's feed channel (and also into the mixing vessel). The solid line represents the measured concentration of the desalted water emerging from the cell. As can be seen (blue curve in Fig. 5), when the cell voltage is applied at $t = 0$ and electrosorption is initiated, we observe a sharp drop in the cell effluent concentration, with this concentration reaching a steady value of roughly 11 mM shortly thereafter. The triangular markers represent the measured electrolyte concentration in the mixing vessel, and this concentration increases upon the application of the cell voltage due to the bead discharge in the mixing vessel. This brine concentration reaches a steady value after roughly three days, at nearly 50 mM. The dashed line is the result of a mass balance, predicting the concentration in the mixing vessel based on the measured salt removed from the feed stream (see ESI† for further details). As can be seen, the mass balance prediction closely matches the measured mixing vessel conductivity, and thus we conclude that approximately all the salt electrosorbed by the beads is released in the mixing vessel and any water transfer through the membrane must have been minor. After three days, both the cell effluent salinity and the mixing vessel salinity have reached steady values, and thus at this time the entire Fbed CDI system is at a steady state while the flow electrodes are recirculating from the mixing vessel to the cell and back. To the best of our knowledge, this is a sole example of a CDI system leveraging suspension electrodes which can perform continuous desalination and closed-loop regeneration and re-use of the electrodes without the need for a second cell[12] or a third membrane.[13] However, we note that in our cell, we are not recovering energy from the discharging beads, which may limit the energy efficiency of the process.

While Fig. 5 shows the performance of our Fbed CDI system under one experimental condition, we demonstrate the performance under a wider variety of conditions in ESI, Fig. S3,† in the form of cell current efficiency. Current efficiency is defined as the molar flux of salt removed from the feedwater divided by the

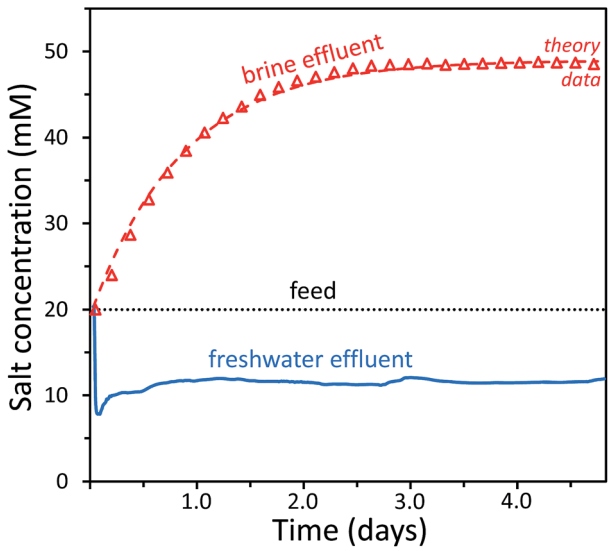

Fig. 5 Representative results for the desalination performance of our Fbed CDI system. The dotted line represents the concentration of the feedwater (20 mM), and the blue line shows the measurement of the cell effluent concentration. The triangular markers show the measured salt concentration in the mixing vessel, and the dashed red line represents the results of a mass balance calculation.

molar flux of electrons transferred between electrodes by the external power supply, and is a widely used metric to quantify the performance of FCDI and electrodialysis cells, as it is directly related to energy efficiency.[1] We show that our cell can achieve near unity charge efficiency for 20 mM feed water under several experimental conditions.

Conclusions

In conclusion, we here present a novel CDI system leveraging fluidized bed electrodes to desalinate water. We show that these electrodes allow for several benefits over previously used flow electrodes, namely a large improvement in flowable electrode CWP from ~20 wt% to 35 wt%, which promises more effective electric charge percolation through the electrode. While the electrode demonstrated a high CWP, simultaneously a low CWP of ~2.5 wt% was maintained in the surrounding flow system, minimizing pump requirements and preventing clogging. We further demonstrated continuous desalination of a feed stream, while regenerating and re-using the electrodes in a simple closed-loop system. Future work will attempt to improve the performance of our Fbed CDI system via engineering modifications, including reducing system response time.

Acknowledgements

This work was supported by the Grand Technion Energy Program (GTEP), and comprises part of The Leona M. and Harry B. Helmsley Charitable Trust reports on Alternative Energy series of the Technion, Israel Institute of Technology, and the Weizmann Institute of Science. GJD would like to acknowledge funding from the Israel National Research Center for Electrochemical Propulsion (INREP). Part of this work was performed in the cooperation framework of Wetsus, European Centre of Excellence for Sustainable Water Technology (www.wetsus.eu). Wetsus is co-funded by the Dutch Ministry of Economic Affairs and Ministry of Infrastructure and Environment, the Province of Fryslân, and the Northern Netherlands Provinces.

References

1 M. Suss, *et al.* Water desalination via capacitive deionization: what is it and what can we expect from it?, *Energy Environ. Sci.*, 2015, **8**, 2296–2319.
2 S. Jeon, *et al.* Desalination via a new membrane capacitive deionization process utilizing flow-electrodes, *Energy Environ. Sci.*, 2013, **6**, 1471.
3 M. Duduta, *et al.* Semi-solid lithium rechargeable flow battery, *Adv. Energy Mater.*, 2011, **1**, 511–516.
4 V. Presser, *et al.* The Electrochemical Flow Capacitor: A New Concept for Rapid Energy Storage and Recovery, *Adv. Energy Mater.*, 2012, **2**, 895–902.
5 B. Kastening, W. Schiel and M. Henschel, Electrochemical polarization of activated carbon and graphite powder: Part I. Capacity of suspensions and polarization dynamics, *J. Electroanal. Chem.*, 1985, **191**, 311–328.
6 S. Porada, *et al.* Carbon flow electrodes for continuous operation of capacitive deionization and capacitive mixing energy generation, *J. Mater. Chem. A*, 2014, **2**, 9313.
7 P. Xu, J. E. Drewes, D. Heil and G. Wang, Treatment of brackish produced water using carbon aerogel-based capacitive deionization technology, *Water Res.*, 2008, **42**, 2605–2617.
8 H. H. Jung, S. W. Hwang, S. H. Hyun, K. H. Lee and G. T. Kim, Capacitive deionization characteristics of nanostructured carbon aerogel electrodes synthesized via ambient drying, *Desalination*, 2007, **216**, 377–385.
9 T. J. Petek, N. C. Hoyt, R. F. Savinell and J. S. Wainright, Characterizing Slurry Electrodes Using Electrochemical Impedance Spectroscopy, *J. Electrochem. Soc.*, 2016, **163**, A5001–A5009.
10 N. C. Hoyt, J. S. Wainright and R. F. Savinell, Mathematical Modeling of Electrochemical Flow Capacitors, *J. Electrochem. Soc.*, 2015, **162**, A652–A657.
11 K. B. Hatzell, M. Boota and Y. Gogotsi, Materials for suspension (semi-solid) electrodes for energy and water technologies, *Chem. Soc. Rev.*, 2015, **44**, 8664–8687.
12 Y. Gendel, A. K. E. Rommerskirchen, O. David and M. Wessling, Batch mode and continuous desalination of water using flowing carbon deionization (FCDI) technology, *Electrochem. Commun.*, 2014, **46**, 152–156.
13 A. Rommerskirchen, Y. Gendel and M. Wessling, Single module flow-electrode capacitive deionization for continuous water desalination, *Electrochem. Commun.*, 2015, **60**, 34–37.
14 S. Jeon, J. Yeo, S. Yang, J. Choi and D. K. Kim, Ion storage and energy recovery of a flow-electrode capacitive deionization process, *J. Mater. Chem. A*, 2014, **2**, 6378.

15 K. B. Hatzell, *et al.* Effect of Oxidation of Carbon Material on Suspension Electrodes for Flow Electrode Capacitive Deionization, *Environ. Sci. Technol.*, 2015, **49**, 3040–3047.
16 J. F. Richardson and W. N. Zaki, Sedimentation and fluidisation: Part I, *Chem. Eng. Res. Des.*, 1997, **75**, S82–S100.
17 J. W. Campos, *et al.* Investigation of carbon materials for use as a flowable electrode in electrochemical flow capacitors, *Electrochim. Acta*, 2013, **98**, 123–130.
18 R. F. Probstein, *Physicochemical hydrodynamics: an introduction*, 2005.